Title
Assessing multimodal optical imaging of perfusion in burn wounds

Journal
Burns, 48(4)

ISSN
0305-4179

Authors
Lertsakdadet, Ben S
Kennedy, Gordon T
Stone, Randolph
et al.

Publication Date
2022-06-01

DOI
10.1016/j.burns.2021.08.026

Available online at www.sciencedirect.com

ScienceDirect

journal homepage: www.elsevier.com/locate/burns

Assessing multimodal optical imaging of perfusion in burn wounds

Ben S. Lertsakdadet [a,b], *Gordon T. Kennedy* [a], *Randolph Stone II* [c], *Christine Kowalczewski* [c], *Andrew C. Kowalczewski* [c], *Shanmugasundaram Natesan* [c], *Robert J. Christy* [c], *Anthony J. Durkin* [a,b], *Bernard Choi* [a,b,d,e,*]

[a] *Beckman Laser Institute and Medical Clinic, University of California, Irvine, CA 92612, USA*
[b] *Department of Biomedical Engineering, University of California, Irvine, CA, 92697, USA*
[c] *United States Army Institute of Surgical Research, 36950 Chambers Pass, Fort Sam Houston, TX 78234, USA*
[d] *Department of Surgery, University of California, Irvine, CA, 92697, USA*
[e] *Edwards Lifesciences Center for Advanced Cardiovascular Technology, University of California, Irvine, CA, 92697, USA*

ARTICLE INFO

Keywords:

Burns
Spatial frequency domain imaging
Laser speckle contrast imaging
Perfusion
Blood flow
Optical properties

ABSTRACT

A critical need exists for early, accurate diagnosis of burn wound severity to help identify the course of treatment and outcome of the wound. Laser speckle imaging (LSI) is a promising blood perfusion imaging approach, but it does not account for changes in tissue optical properties that can occur with burn wounds, which are highly dynamic environments. Here, we studied optical property dynamics following burn injury and debridement and the associated impact on interpretation of LSI measurements of skin perfusion. We used spatial frequency domain imaging (SFDI) measurements of tissue optical properties to study the impact of burn-induced changes in these properties on LSI measurements. An established preclinical porcine model of burn injury was used (n = 8). SFDI and LSI data were collected from burn wounds of varying severity. SFDI measurements demonstrate that optical properties change in response to burn injury in a porcine model. We then apply theoretical modeling to demonstrate that the measured range of optical property changes can affect the interpretation of LSI measurements of blood flow, but this effect is minimal for most of the measured data. Collectively, our results indicate that, even with a dynamic burn wound

Abbreviations: A, constant dependent on boundary conditions; AAALAC, Association for Assessment and Accreditation of Laboratory Animal Care; CCD, charge-coupled device; D_B, Brownian diffusion coefficient; FDA, Food and Drug Administration; FOV, field of view; G_1, intensity autocorrelation function; IACUC, Institutional Animal Care and Use Committee; K, speckle contrast; k_0, wavenumber of light; LSI, laser speckle imaging; n, refractive index; P_0, incident optical power; q, laser source intensity; ROI, region of interest; SFDI, spatial frequency domain imaging; SFI, speckle flow index; T, exposure time; USAISR, United States Army Institute for Surgical Research; $\langle I \rangle$, mean intensity; $\langle \Delta r^2(\tau) \rangle$, mean square displacement; β, factor accounting for polarization and speckle/pixel size ratio; λ, laser wavelength; μ_a, absorption coefficient; $\mu_{a,dyn}$, dynamic optical property term; μ_{eff}, effective attenuation coefficient; μ_s', reduced scattering coefficient; μ_{tr}, transport coefficient; σ, standard deviation of laser intensity.

* *Corresponding author at*: Beckman Laser Institute and Medical Clinic, University of California, Irvine, CA 92612, USA.
E-mail addresses: blertsak@uci.edu (B.S. Lertsakdadet), gtkenned@uci.edu (G.T. Kennedy), randolph.stone4.civ@mail.mil (R. Stone), christine.j.kowalczewski.ctr@mail.mil (C. Kowalczewski), andrewkowalczewski@gmail.com (A.C. Kowalczewski), shanmugasundaram.natesan.ctr@mail.mil (S. Natesan), robert.j.christy12.civ@mail.mil (R.J. Christy), adurkin@uci.edu (A.J. Durkin), choib@uci.edu (B. Choi).

https://doi.org/10.1016/j.burns.2021.08.026

environment, blood-flow measurements with LSI can serve as an appropriate strategy for accurate assessment of burn severity.

1. Introduction

Worldwide, more than 10 million people annually suffer from burn wounds that receive medical attention [1]. The American Burn Association approximates 450,000 burn injuries occur each year in the United States alone [2]. Historically, burns have constituted 5–20% of conventional warfare casualties [3]. Burn wounds can be classified into superficial, superficial partial, deep partial, and full thickness burns. Superficial burn wounds are minor and will heal on their own, whereas full thickness burns benefit from surgical intervention [4]. Partial thickness burns may progress into deep partial thickness burns, making them more challenging to assess and treat appropriately [5].

The dynamic nature of burn wounds within the first 24–72 h makes them extremely difficult to diagnose accurately [6]. Current clinical protocols for classifying burn wounds are based on visual observations by an experienced surgeon [5,7,8]. Experienced surgeons are accurate at assessing burn depth only 64%–76% of the time [9]. Therefore, a critical need exists for early, accurate diagnosis of burn wound severity to help identify the course of treatment and outcome of the wound [10–12].

Various optical imaging modalities have been utilized to measure burn severity. Two promising candidates are laser speckle imaging (LSI), which measures tissue perfusion, and spatial frequency domain imaging (SFDI), which measures tissue absorption and scattering properties. LSI uses diffuse laser light to illuminate the entire sample [4,13–17] and measurements of the fluctuation in the intensity of the reflected light in a single snapshot [18]. LSI has shown promise in improving upon clinical assessment of burn wounds [4,14,19]. Also, the perfusion units of LSI, in Speckle Flow Index (SFI), have been shown to correlate linearly with blood flow rates found in tissue [20].

Although studies have shown that blood perfusion is an adequate method for assessing burn wounds, they do not consider the associated structural changes. A non-contact imaging modality capable of quantifying these structural changes is spatial frequency domain imaging (SFDI). SFDI is an imaging technique that provides optical properties of tissue, such as reduced scattering coefficient, μ_s', and absorption coefficient, μ_a [21–26]. Ponticorvo et al. [27] used μ_s' from SFDI and perfusion units from LSI to categorize burns. They showed that at 24 h after burn, LSI provided a sensitivity and specificity of 66% and 90%, respectively. At 72 h, sensitivity improved to 100%, but specificity decreased to 58%. They also showed that SFDI provided a sensitivity and specificity of 93% and 74% at 24 h, and 83% and 90% at 72 h.

LSI is a relative blood perfusion method that does not account for changes in tissue optical properties. Burn wounds are highly dynamic environments, with changes in local blood volume [5] and architecture. These changes likely confound blood flow measurements with LSI. By incorporating SFDI, we can investigate the impact of optical property dynamics on the perfusion measured by LSI.

Here, we first demonstrate that optical properties change in response to burn injury in a porcine model. We use modeling to demonstrate that the measured range of optical property changes can affect the interpretation of LSI measurements of blood flow, but this effect is minimal for most of the measured data. Together, these results indicate that blood-flow measurements with laser speckle imaging may serve as an appropriate strategy for accurate assessment of burn severity.

2. Materials and methods

2.1. Animals

All experiments were carried out under a US Army Institute for Surgical Research (USAISR) approved IACUC protocol. Research was conducted in compliance with the Animal Welfare Act, the implementing Animal Welfare regulations, and the principles of the Guide for the Care and Use of Laboratory Animals, National Research Council. The facility's Institutional Animal Care and Use Committee approved all research conducted in this study. The facility where this research was conducted is fully accredited by the AAALAC. Animals were housed individually in a temperature-controlled environment with a 12-h light/dark cycle in the AAALAC approved vivarium at the USAISR with access to water and food ad libitum. Before burning, hair was removed from the dorsum of the animals, tattoos were created around each wound, and the skin was rinsed with sterile water.

2.2. Varying-burn depth and varying-depth of debridement

Each anesthetized pig received 10 burns (5 cm × 5 cm) created on their dorsal side spaced roughly 3 cm from the spine in two evenly distributed rows. The wounds varied in burn severity from superficial to full thickness, followed by varying depths of skin debridement. Burn treatments were randomized and induced on the dorsal side of each pig. Each pig received ten burn treatments. The contact burn device used was a 5 cm × 5 cm brass burn tool heated to 100 °C with active temperature control [28]. LSI and SFDI data were acquired pre- and post-burn on Day 0 of the study. On Day 7 of the study, debridement of the wound bed was performed with a pneumatic dermatome set to 0.030″, and LSI and SFDI data were acquired pre- and post-debridement. The depths of debridement varied from 1 pass (0.030″) to 4 passes (0.120″) with the dermatome.

In addition to the ten burns, two control sites were located adjacent to the first and last burns for each pig. A total of 8 pigs were included in this study resulting in LSI and SFDI data on 80 experimental and 16 control sites for processing and data

analysis. To focus on assessment of acute burn severity, we only did not include data collected after initial debridement. The time points of interest for this study were Day 0 pre- and post-burn and Day 7 pre- and post-debridement due to the relatively large changes in optical properties and blood flow expected at these time points.

2.3. *Spatial frequency domain imaging*

To measure skin optical properties, we used a commercial FDA-approved SFDI device (ReflectRS, Modulim, Irvine, CA). Cuccia et al. [29] describe in detail SFDI theory. Briefly, SFDI uses structured illumination at different spatial frequencies (typically sine waves, although square waves also can be used, combined with theoretical modeling of light propagation in tissue, to estimate maps of absorption and reduced scattering coefficients [30]. With measurements collected at multiple excitation wavelengths, spectral analysis can extract maps of tissue chromophores such as oxy- and deoxyhemoglobin.

The SFDI consisted of an imaging head mounted to a mobile cart with an articulating arm. The device provides a field of view (FOV) of 20 cm × 15 cm from a height of 32 cm from the

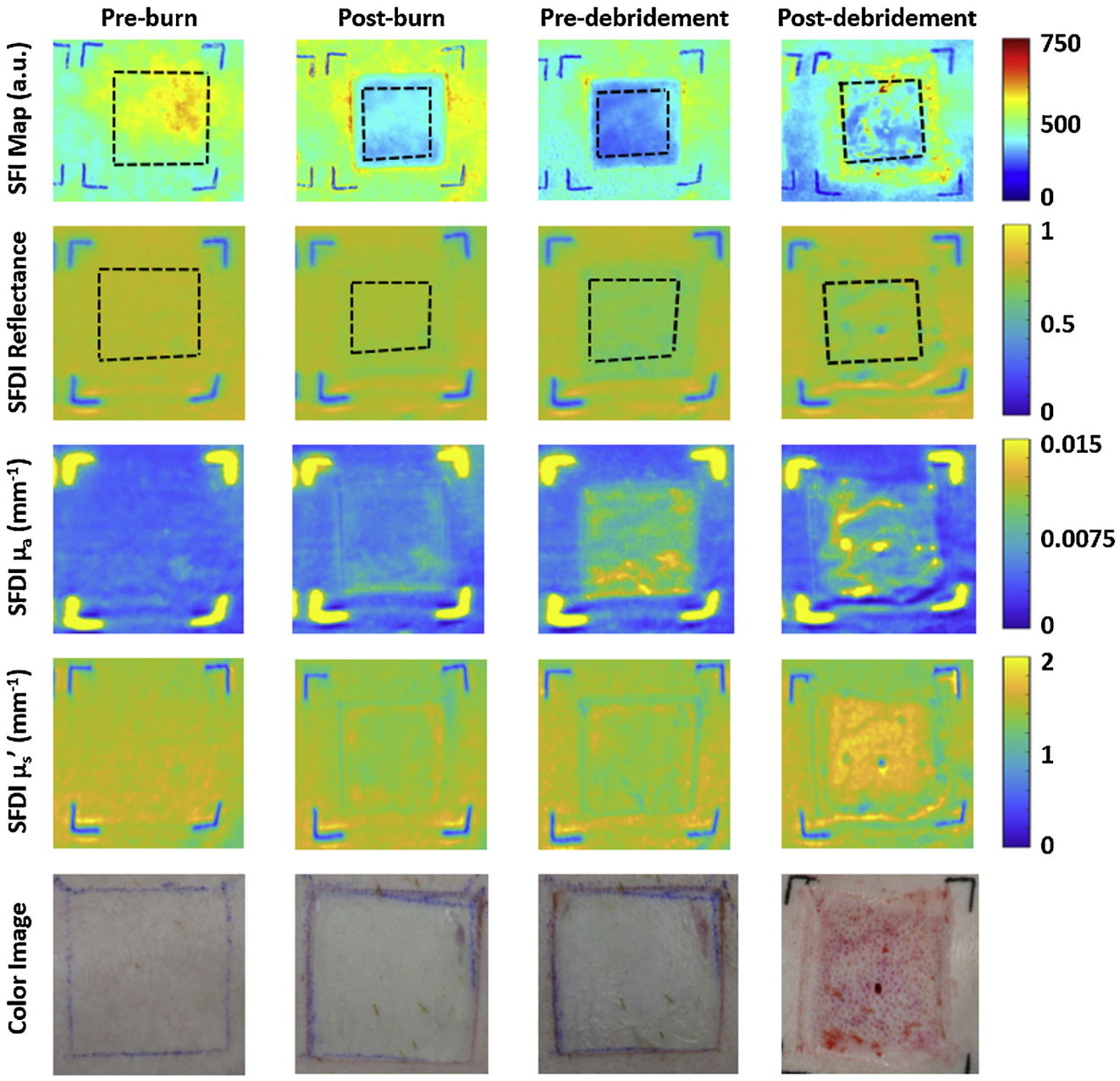

Fig. 1 – LSI and SFDI maps of a single burn treatment. Speckle Flow Index (SFI), SFDI reflectance, reduced scattering coefficient (μ_s'), and absorption coefficient (μ_a) maps of a single treatment site pre- and post-burn and debridement are shown. The regions of interest (ROI) shown in black were manually selected in an attempt to obtain similar areas of tissue. The ROI selected for the SFDI reflectance map was applied to the μ_s' and μ_a maps. Color photographs are shown for each of the four stages to provide a visual representation of the sites.

sample. Images were acquired using the MI Acquire V1.34.00 software, and the device was set to acquire 3 data sets of each sample. Each data set consisted of 8 wavelengths from 471 nm to 851 nm with five sinusoidal spatial frequencies, evenly spaced between 0 mm^{-1} and 0.2 mm^{-1}. The resulting data sets were used to produce the reduced scattering coefficient (μ_s') and absorption coefficient (μ_a) images used for this study (Fig. 1). We selected a region of interest (ROI) using the μ_s' and μ_a images for each treatment site (Fig. 1). We quantified the mean μ_s' and μ_a within these ROIs using interpolation for 808 nm to correspond with the laser wavelength used in the LSI device.

2.4. Laser speckle imaging device

The laser speckle imaging (LSI) system used in this study consisted of an imaging head mounted to a mobile cart with an articulating arm. The imaging head consisted of an 8-bit, 1.32 megapixel CCD camera (CMLN-13S2M-CS, FLIR Integrated Imaging Solutions, Inc., Richmond, BC, Canada), a variable zoom C-mount lens (Computar C-Mount 13–130 mm Varifocal Lens, Computar), and 808 nm near-infrared laser diode (140 mW, Ondax Inc., Monrovia, CA). A 785 nm long-pass filter was placed in front of the CCD sensor to allow data acquisition with room lights. A 750 nm–850 nm linear polarizer (Edmund Optics) was placed in front of the variable zoom lens to remove specular reflectance from the surface of the sample.

The device provided a FOV of approximately 14 cm × 10.5 cm at a working distance of 35 cm from the sample. Each data set contained 150 raw images acquired at 15 Hz. All raw images were converted into speckle contrast (K) images using a 7 × 7 sliding window and the relationship of $K = \sigma/\langle I\rangle$, where σ is the standard deviation and $\langle I\rangle$ is the mean intensity of all pixels within the window. All speckle contrast images from each data set were used to create an average speckle contrast image. The speckle contrast images were also converted into speckle flow index (SFI) images to show relative blood flow, using the relationship of $SFI = 1/(2TK^2)$, where T is the camera exposure time in seconds. SFI is a measure of arbitrary units (a.u.). An ROI comparable to the ones selected for the μ_s' and μ_a was selected using the average speckle contrast image (Fig. 1). We quantified the mean K and SFI within the ROI.

2.5. Modeling

A common approximation that describes light transport in scattering media, such as biological tissues, is the diffusion approximation [31,32]. A similar correlation diffusion approximation [33] is used to describe momentum transport that occurs due to interactions with moving scattering particles, such as red blood cells:

$$\nabla^2 G_1(\tau) - \mu_{eff} G_1(\tau) = q \tag{1}$$

where $G_1(\tau)$ is the intensity autocorrelation function, μ_{eff} is the effective attenuation coefficient of the medium [mm^{-1}], and q is the laser source intensity.

For uniform planar illumination, the speckle contrast (K) is related to G_1 as [34]:

$$K = \sqrt{\frac{\frac{2}{T}\int_0^T \beta G_1^2(\tau)(1-\tau/T)d\tau}{G_1^2(\tau=0)}} \tag{2}$$

where β accounts for polarization and speckle/pixel size ratio, and

$$G_1(\tau) = \frac{3P_0 A\frac{\mu_s'}{\mu_{tr}}}{\left(\frac{\mu_{eff}(\tau)}{\mu_{tr}}+1\right)\left(\frac{\mu_{eff}(\tau)}{\mu_{tr}}+3A\right)} \tag{3}$$

where P_0 is the incident optical power and $\mu_{tr} = \mu_a + \mu_s'$ is the transport coefficient. A is a constant that depends on the assumed boundary conditions used in the simulation of light transport in the medium. For a partial current boundary condition, A is

$$A = \frac{1 - R_{eff}}{2\left(1 + R_{eff}\right)} \tag{4}$$

and

$$R_{eff} = 0.0636n + 0.668 + \frac{0.710}{n} - \frac{1.440}{n^2} \tag{5}$$

where n is the refractive index of the skin (assumed to be 1.4).

The effective attenuation coefficient describing dynamic light scattering is given as

$$\mu_{eff}(\tau) = \sqrt{3\mu_{a,dyn}(\tau)\mu_{tr}} \tag{6}$$

We previously described a dynamic optical property term $\mu_{a,dyn}$ that accounts for both the light absorption properties of the tissue and particle motion [34]:

$$\mu_{a,dyn}(\tau) = \mu_a + \frac{1}{3}\mu_s' k_o^2 \langle\langle \Delta r^2(\tau)\rangle\rangle \tag{7}$$

where k_o is the wavenumber of light, $k_o = 2n/\lambda$, λ is the laser wavelength [m], and $\langle\Delta r^2(\tau)\rangle$ is the mean square displacement of the dynamic scattering particles.

Here, we describe $\Delta r^2(t)$ as a Brownian motion term:

$$\langle\langle \Delta r^2(\tau)\rangle\rangle = 6D_{BT} \tag{8}$$

where D_B is the Brownian diffusion coefficient [m^2/s]. This approach is consistent with that used in diffuse correlation spectroscopy [35] and diffuse speckle contrast analysis [36] for describing interactions between light and red blood cells primarily in capillaries.

Hence, with optical property measurements from SFDI and speckle contrast measurements from LSI, we use Eqs. (2)–(8) to estimate D_B. Specifically, we set up an iterative solver in a Microsoft Excel spreadsheet to perform the following steps:

(a) We first calculated $\langle\Delta r^2(\tau)\rangle$ for an assumed value of D_B and different values of τ using Eq. (8).

(b) The measured values of μ_a and μ_s' and calculated values of $<\Delta r^2(\tau)>$ and k_o were used to calculate $\mu_{a,dyn}(\tau)$ for the same values of τ with Eq. (7)
(c) The resultant $\mu_{a,dyn}$ and μ_{tr} values were used to calculate μ_{eff} for each value of τ using Eq. (6).
(d) Eqs. (4) and (5) were used to calculate A
(e) The values from (a) to (d) were used to calculate $G_1(\tau)$ for different values of τ. The value of P_0 was not important because it canceled out in Eq. (2).
(f) Using Eq. (2), the value of K was calculated using numerical integration of $G_1(\tau)$.
(g) This process was repeated in an iterative fashion with different input values of D_B until a simulated SFI value was reached that matched the measured value, at integer precision.

In this work, we first modeled the potential effects of optical properties on the interpretation of K as a measure of blood flow. We used the optical property and K values measured from the porcine burn experiments to define the ranges of values explored with modeling. We then calculated D_B values for all measured combinations of optical properties and speckle contrast. We performed a linear regression analysis to study the impact of measured optical property variations on our interpretation of speckle contrast to measure blood flow.

3. Results

3.1. *Both optical properties and speckle-based measurements of blood flow change in response to burn injury (Fig. 2)*

The optical properties of the porcine skin at each given time point varied considerably. The typical assumed optical properties for absorption and reduced scattering coefficients of skin are 0.01 mm^{-1} and 1 mm^{-1}, respectively, at a wavelength of ~808 nm. However, the median values of our measurements across all time points for absorption, reduced scattering coefficient and speckle flow index were 0.0075 mm^{-1}, 1.4 mm^{-1}, and 400.

The pre- and post-burn data were treated as paired data sets and the μ_a and μ_s' values were significantly different ($p < 0.05$). However, the μ_a and μ_s' values for paired pre-and post-debridement were not significantly different ($p = 0.31$ and $p = 0.10$, respectively).

3.2. *Optical property changes affect interpretation of SFI as a blood-flow metric (Fig. 3)*

Diffusion coefficient (D_B) is a characteristic metric used to represent tissue perfusion, and effects of optical property variations among individuals and within an individual over time are taken into account. Across the range of values observed for μ_s' at the pre- and post-burn and debridement time points, the D_B values differed by less than 10% at each SFI value modeled ($9.1 \pm 0.4\%$). The D_B values differed by $43 \pm 1.1\%$ at each SFI value across the range of values observed for μ_a. The change in μ_a has a greater contribution to the D_B value than μ_s'.

3.3. *Even with dynamic optical properties following burn injury, changes in blood flow are well represented by measured changes in SFI (Fig. 4)*

The SFI values of skin perfusion and estimated diffusion coefficients were compared from SFDI and LSI measurements collected at all time points. For all paired values, a strong linear relationship ($R^2 = 0.87$) exists between D_B and SFI. A high (84%) percentage of all measured SFI values were less than 500. For SFI values greater than 500, the relationship between D_B and SFI has more scatter and hence a weaker goodness of fit ($R^2 = 0.56$) with linear regression analysis.

4. Discussion

Our results reveal that the range of optical property changes associated with burn injury can affect the interpretation of SFI as a blood-flow metric, but for the majority of burns presented in this study, changes in blood flow are well represented by measured changes in SFI. Burn wounds are difficult to

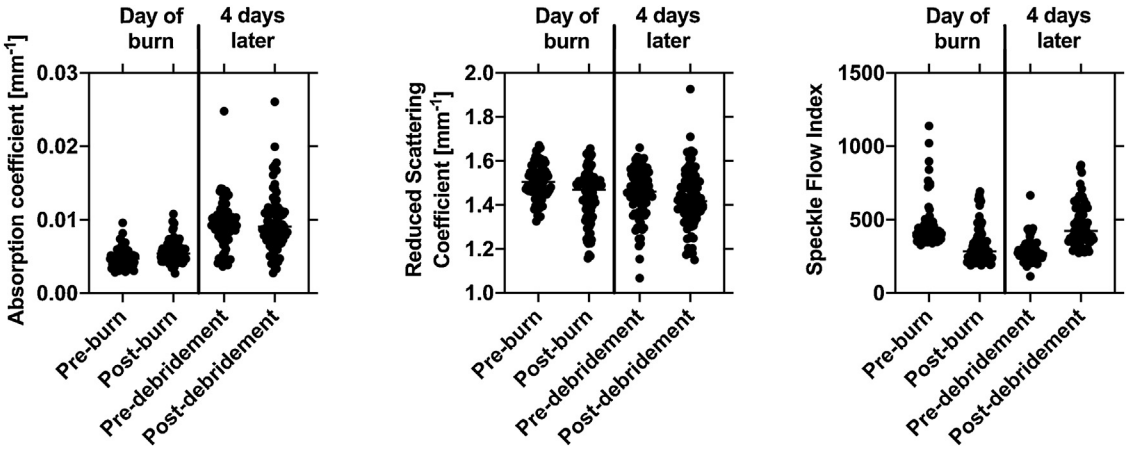

Fig. 2 – Optical properties and speckle flow index values pre- and post-burn and debridement.

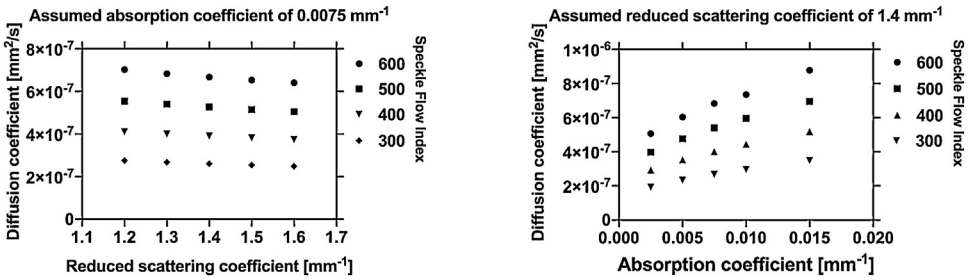

Fig. 3 – Resulting diffusion coefficient (D_B) with respect to varying speckle flow index values across the range of observed values for reduced scattering coefficient (μ_s') and absorption coefficient (μ_a). Eqs. (2)–(8) were used to estimate D_B from measured values of μ_a, μ_s', and SFI shown in Fig. 2. (Left) Assuming a median μ_a value of 0.0075 mm^{-1}, the model predicts that the mapping between SFI and D_B is minimally affected by changes in μ_s'. (Right) Assuming a median μ_s' value of 1.4 mm^{-1}, the model predicts that the mapping between SFI and D_B is affected by changes in μ_a. These data collectively suggest that speckle-based measurements of flow can be affected by changes in tissue μ_a.

accurately assess due to their dynamic nature in the first 24–72 h after burn [5]. Hemodynamic changes and optical property changes occur as the wound may convert into more severe burns or begin to heal over time. Reducing the time after injury to the correct diagnosis is of benefit to improve the prognosis of the wound [14,24,37]. Imaging modalities, such as LSI and SFDI, have attempted to provide clinicians with an objective and quantifiable method to diagnose burn wounds.

LSI has shown its potential to provide meaningful blood flow information in assessing burn wound severity. Ponticorvo et al. [14] showed that at 24 and 72 h after burn, LSI correctly assessed burn severity in 36 of 48 burn sites (75%) and 40 of 48 burn sites (83%), respectively. Mirdell et al. [19] also showed sensitivities and specificities of 92% and 78% at 24 h and 100% and 90% at 96 h post-burn.

SFDI and LSI have been used to measure optical properties and blood flow, respectively, in multiple published studies [14,24,27,37–40]. With SFDI, μ_s' values decrease soon after burns are induced [4,24,38,40]. Mazhar et al. [38] observed that μ_a did not change immediately after burn, but showed a progressive increase in μ_a over a three-day period after burn, associated with an increase in total hemoglobin content. For both superficial and deep partial thickness burn wounds, SFI values also decrease immediately [4,39]. The trends observed in our data are in agreement with these published reports. Here, we also report on optical property and SFI changes due to debridement (Fig. 2). The absorption coefficient and SFI values are higher after debridement, presumably due to exposure of viable, vascularized skin regions. Collectively, these data demonstrate consistent changes in optical properties and SFI values at various time points after burn.

Using a theoretical framework first described by Boas and Yodh [33] for dynamic light scattering, Mazhar et al. [34] describe speckle contrast as a function of particle motion (as D_B) and optical properties. Optical properties have a clear effect on K, and hence SFI. An increase in μ_a or μ_s' is associated with increased SFI due to a decrease in optical pathlength and hence decreased number of interactions with moving particles. A given percent change in μ_a has a larger impact on K than the same change in μ_s'. Here, we demonstrate this trend for the range of optical properties and SFI values measured from our porcine burn model (Fig. 3). As an illustrative example: if SFI is 500 for a μ_a of 0.0075 mm^{-1}, the corresponding D_B is 5.4×10^{-7} mm^2/s. If SFI

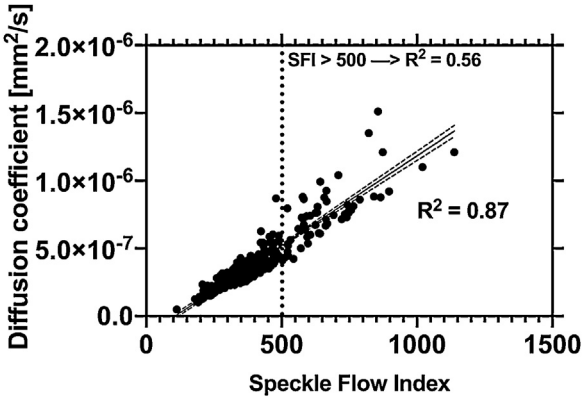

Fig. 4 – Quantified diffusion coefficient (D_B) with respect to speckle flow index (SFI). There exists a strong linear relationship between D_B and SFI ($R^2 = 0.87$), with an increase in scatter for SFI values greater than 500. The slope is 1.324×10^{-9} {95% CI: [1.269×10^{-9},1.37×10^{-9}]} and the y-intercept -1.4×10^{-7}.

increases to 600, the new D_B is 6.84 × 10^{-7} mm^2/s. However, if this increase is accompanied by an increase in μ_a to 0.015 mm^{-1}, perhaps due to inflammation, then the new D_B is 8.78 × 10^{-7} mm^2/s, or a 63% increase. With this simple example, use of SFI alone underestimates the actual change in the blood flow by 3×. Collectively, these data suggest that optical property dynamics can play a large role in our interpretation of LSI measurements.

However, with application of the correlation diffusion equation and SFDI measurements of optical properties to analysis of measurements of K, we observe that a strong linear relationship exists between SFI measurements and corresponding D_B values (Fig. 4). This result strongly suggests that, despite the range of skin optical properties associated with burn wounds of different severities, LSI is a reasonably accurate measurement tool for blood flow assessment. SFI values greater than 500 were measured for 16% of the measurements. For these measurements, the R^2 associated with the linear regression is lower, suggesting that optical properties may have a larger effect on the SFI measurements. In addition, we [20] previously showed that the relationship between SFI and flow speed deviates from linearity at higher flow speeds. The linear response range of SFI to flow speed depends on camera exposure time. We postulate that the linear relationship between D_B and SFI may become weaker at the higher SFI values measured in this study, thus contributing to the observed increase in deviation of the data from the linear regression model. Nevertheless, these data collectively demonstrate for the first time, to the best of our knowledge, that LSI measurements from a highly dynamic system such as burn wound healing, are reasonably accurate indices of blood flow.

Limitations in our study exist. Here, we present functional optical data collected from a collection of burn injuries without discussion of burn severity. Although specific burn severities were intended based on changing contact time of the heating element, we acknowledge that actual burn severity can be assessed only with histological analysis, which is forthcoming. In this study, we used two separate systems for imaging which caused some delays between acquiring SFDI and LSI data. To address this, future studies utilizing a co-registered SFDI and LSI system would allow us to acquire both data simultaneously and pixel-to-pixel correction of optical properties and SFI [23]. This co-registered system would also allow the quantification of metabolic rate of oxygen consumption in burn wounds and provide additional information in the burn dynamics. Finally, we present data collected with an established control model of burn injury. With this model, we observed optical property values that showed considerable variability (Fig. 1). We speculate that the measured ranges of μ_a and μ_s' would include values that would be observed with other models of burn injury. Additional data collection with other burn models is warranted.

In summary, our results demonstrate that burn wounds induce considerable variation in skin optical properties, which in turn can affect speckle contrast. However, even with these changes in optical properties, our study results suggest that LSI measurements accurately reflect changes in blood flow, and thus may serve as a reliable measure of skin viabilityafter burn.

Funding

This material is funded in part by the Arnold and Mabel Beckman Foundation. In addition, this material is based upon work supported by the Air Force Office of Scientific Research under award numbers FA9550-17-1-0193, FA9550-20-1-0052, FA9550-14-1-0034, and FA9550-16-1-0342]. Research reported in this publication was also supported by the National Institutes of Biomedical Imaging and Bioengineering (NIBIB) and the National Center for Advancing Translational Sciences (NCATS) of the National Institutes of Health under award numbers P41EB015890 and TL1TR001415, respectively. This research was also supported in part by the Medical Research and Development Command and an appointment to the Postgraduate Research Participation Program at the U.S. Army Institute of Surgical Research (USAISR) administered by the Oak Ridge Institute for Science and Education through an interagency agreement between the U.S. Department of Energy and USAISR. Per NIH reporting instructions, we report the estimated percent and dollar amounts of the project financed with Federal money are 100% and $49,500, respectively.

Conflict of interest

Except for AJD, the authors declare that they have no known competing financial interests or personal relationships that could have appeared to influence the work reported in this paper. AJD is a co-founder of Modulated Imaging, Inc (current name: Modulim). However, he does not have any active role in that company and is in compliance with University of California, Irvine and NIH policies regarding conflicts of interest.

Acknowledgements

The content is solely the responsibility of the authors and does not necessarily represent the official views of the NCATS, NIBIB, or NIH. Any opinions, finding, and conclusions or recommendations expressed in this material are those of the authors and do not necessarily reflect the views of the United States Air Force. The opinions and assertions contained herein are the private views of the authors and are not to be construed as official or reflecting the views of the Department of Defense or Department of Army. RS and RJC are employees of the U.S. Government, and this work was prepared as part of their official duties.

REFERENCES

[1] World Health Organization. The global burden of disease: 2004 update, https://www.who.int/healthinfo/global_burden_disease/2004_report_update/en/. [Accessed 5 January 2021].
[2] American Burn Association. Burn Injury Fact Sheet. 2018. . . [Accessed 5 January 2021] https://ameriburn.org/wp-content/uploads/2017/12/nbaw-factsheet_121417-1.pdf.

[3] Cancio LC, Horvath EE, Barillo DJ, Kopchinski BJ, Charter KR, Montalvo AE, et al. Burn support for Operation Iraqi Freedom and related operations, 2003 to 2004. J Burn Care Rehabil 2005;26:151–61, doi:http://dx.doi.org/10.1097/01.bcr.0000155540.31879.fb.
[4] Ponticorvo A, Burmeister DM, Yang B, Choi B, Christy RJ, Durkin AJ. Quantitative assessment of graded burn wounds in a porcine model using spatial frequency domain imaging (SFDI) and laser speckle imaging (LSI). Biomed Opt Express 2014;5:3467–81, doi:http://dx.doi.org/10.1364/BOE.5.003467.
[5] Shupp JW, Nasabzadeh TJ, Rosenthal DS, Jordan MH, Fidler P, Jeng JC. A review of the local pathophysiologic bases of burn wound progression. J Burn Care Res 2010;31:849–73, doi:http://dx.doi.org/10.1097/BCR.0b013e3181f93571.
[6] Hoeksema H, Van de Sijpe K, Tondu T, Hamdi M, et al. Accuracy of early burn depth assessment by laser Doppler imaging on different days post burn. Burns 2009;35:36–45, doi:http://dx.doi.org/10.1016/j.burns.2008.08.011.
[7] Heimbach D, Engrav L, Grube B, Marvin J. Burn depth: a review. World J Surg 1992;16:10–5, doi:http://dx.doi.org/10.1007/BF02067108.
[8] Singh V, Devgan L, Bhat S, Milner SM. The pathogenesis of burn wound conversion. Ann Plast Surg 2007;59:109–15, doi:http://dx.doi.org/10.1097/01.sap.0000252065.90759.e6.
[9] Jaskille AD, Shupp JW, Jordan MH, Jeng JC. Critical review of burn depth assessment techniques: Part I. Historical review. J Burn Care Res 2009;30:937–47, doi:http://dx.doi.org/10.1097/BCR.0b013e3181c07f21.
[10] Davis SC, Mertz PM, Bilevich ED, Cazzaniga AL, Eaglstein WH. Early debridement of second-degree burn wounds enhances the rate of epithelization—an animal model to evaluate burn wound therapies. J Burn Care Rehabil 1996;17:558–61, doi:http://dx.doi.org/10.1097/00004630-199611000-00014.
[11] Eski M, Ozer F, Firat C, Alhan D, Arslan N, Senturk T, et al. Cerium nitrate treatment prevents progressive tissue necrosis in the zone of stasis following burn. Burns 2012;38:283–9, doi:http://dx.doi.org/10.1016/j.burns.2011.08.008.
[12] Firat C, Samdanci E, Erbatur S, Aytekin AH, Ak M, Turtay MG, et al. β-Glucan treatment prevents progressive burn ischaemia in the zone of stasis and improves burn healing: an experimental study in rats. Burns 2013;39:105–12, doi:http://dx.doi.org/10.1016/j.burns.2012.02.031.
[13] Briers JD, Webster S. Laser speckle contrast analysis (LASCA): a nonscanning, full-field technique for monitoring capillary blood flow. J Biomed Opt 1996;1:174–9, doi:http://dx.doi.org/10.1117/12.231359.
[14] Ponticorvo A, Burmeister DM, Rowland R, Baldado M, Kennedy GT, Saager R, et al. Quantitative long-term measurements of burns in a rat model using Spatial Frequency Domain Imaging (SFDI) and Laser Speckle Imaging (LSI). Lasers Surg Med 2017;49:293–304, doi:http://dx.doi.org/10.1002/lsm.22647.
[15] Yang O, Choi B. Laser speckle imaging using a consumer-grade color camera. Opt Lett 2012;37:3957–9, doi:http://dx.doi.org/10.1364/OL.37.003957.
[16] Yang B, Yang O, Guzman J, Nguyen P, Crouzet C, Osann KE, et al. Intraoperative, real-time monitoring of blood flow dynamics associated with laser surgery of port wine stain birthmarks. Lasers Surg Med 2015;47:469–75, doi:http://dx.doi.org/10.1002/lsm.22369.
[17] Lertsakdadet B, Yang BY, Dunn CE, Ponticorvo A, Crouzet C, Bernal N, et al. Correcting for motion artifact in handheld laser speckle images. J Biomed Opt 2018;23:1–7, doi:http://dx.doi.org/10.1117/1.JBO.23.3.036006.
[18] Boas DA, Dunn AK. Laser speckle contrast imaging in biomedical optics. J Biomed Opt 2010;15:011109, doi:http://dx.doi.org/10.1117/1.3285504.
[19] Mirdell R, Farnebo S, Sjöberg F, Tesselaar E. Accuracy of laser speckle contrast imaging in the assessment of pediatric scald wounds. Burns 2018;44:90–8, doi:http://dx.doi.org/10.1016/j.burns.2017.06.010.
[20] Choi B, Ramirez-San-Juan JC, Lotfi J, Stuart Nelson J. Linear response range characterization and in vivo application of laser speckle imaging of blood flow dynamics. J Biomed Opt 2006;11:041129, doi:http://dx.doi.org/10.1117/1.2341196.
[21] Cuccia DJ. Spatial frequency domain imaging (SFDI): a technology overview and validation of an LED-based clinic friendly device. Proc SPIE 2012;8254:825405, doi:http://dx.doi.org/10.1117/12.908860.
[22] O'Sullivan TD, Cerussi AE, Cuccia DJ, Tromberg BJ. Diffuse optical imaging using spatially and temporally modulated light. J Biomed Opt 2012;17:071311, doi:http://dx.doi.org/10.1117/1.JBO.17.7.071311.
[23] Ghijsen M, Lentsch GR, Gioux S, Brenner M, Durkin AJ, Choi B, et al. Quantitative real-time optical imaging of the tissue metabolic rate of oxygen consumption. J Biomed Opt 2018;23:1–12, doi:http://dx.doi.org/10.1117/1.JBO.23.3.036013.
[24] Nguyen JQ, Crouzet C, Mai T, Riola K, Uchitel D, Liaw LH, et al. Spatial frequency domain imaging of burn wounds in a preclinical model of graded burn severity. J Biomed Opt 2013;18:66010, doi:http://dx.doi.org/10.1117/1.JBO.18.6.066010.
[25] Gioux S, Mazhar A, Cuccia DJ, Durkin AJ, Tromberg BJ, Frangioni JV. Three-dimensional surface profile intensity correction for spatially modulated imaging. J Biomed Opt 2009;14:034045, doi:http://dx.doi.org/10.1117/1.3156840.
[26] Erickson TA, Mazhar A, Cuccia D, Durkin AJ, Tunnell JW. Lookup-table method for imaging optical properties with structured illumination beyond the diffusion theory regime. J Biomed Opt 2010;15:036013, doi:http://dx.doi.org/10.1117/1.3431728.
[27] Ponticorvo A, Rowland R, Baldado M, Burmeister DM, Christy RJ, Bernal NP, et al. Evaluating clinical observation versus Spatial Frequency Domain Imaging (SFDI), Laser Speckle Imaging (LSI) and thermal imaging for the assessment of burn depth. Burns 2019;45:450–60, doi:http://dx.doi.org/10.1016/j.burns.2018.09.026.
[28] Stone R, Jockheck-Clark AR, Natesan S, Rizzo JA, Wienandt NA, et al. Enzymatic debridement of porcine burn wounds via a novel protease, SN514. J Burn Care Res 2020;41:1015–28, doi:http://dx.doi.org/10.1093/jbcr/iraa111.
[29] Cuccia DJ, Bevilacqua F, Durkin AJ, Ayers FR, Tromberg BJ. Quantitation and mapping of tissue optical properties using modulated imaging. J Biomed Opt 2009;14:024012, doi:http://dx.doi.org/10.1117/1.3088140.
[30] Nadeau KP, Rice TB, Durkin AJ, Tromberg BJ. Multifrequency synthesis and extraction using square wave projection patterns for quantitative tissue imaging. J Biomed Opt 2015;20:116005, doi:http://dx.doi.org/10.1117/1.JBO.20.11.116005.
[31] Ishimaru A. Diffusion of light in turbid material. Appl Opt 1989;28:2210–5, doi:http://dx.doi.org/10.1364/AO.28.002210.
[32] Jacques SL, Pogue BW. Tutorial on diffuse light transport. J Biomed Opt 2008;13:041302, doi:http://dx.doi.org/10.1117/1.2967535.
[33] Boas DA, Yodh AG. Spatially varying dynamical properties of turbid media probed with diffusing temporal light correlation. J Opt Soc Am A 1997;14:192–215, doi:http://dx.doi.org/10.1364/JOSAA.14.000192.
[34] Mazhar A, Cuccia DJ, Rice TB, Carp SA, Durkin AJ, Boas DA, et al. Laser speckle imaging in the spatial frequency domain. Biomed Opt Express 2011;2:1553–63, doi:http://dx.doi.org/10.1364/BOE.2.001553.
[35] Durduran T, Zhou C, Buckley EM, Kim MN, Yu G, Choe R, et al. Optical measurement of cerebral hemodynamics and oxygen metabolism in neonates with congenital heart defects. J Biomed Opt 2010;15:037004, doi:http://dx.doi.org/10.1117/1.3425884.

[36] Bi R, Dong J, Lee K. Deep tissue flowmetry based on diffuse speckle contrast analysis. Opt Lett 2013;38:1401–3, doi:http://dx.doi.org/10.1364/OL.38.001401.
[37] Burmeister DM, Ponticorvo A, Yang B, Becerra SC, Choi B, Durkin AJ, et al. Utility of spatial frequency domain imaging (SFDI) and laser speckle imaging (LSI) to non-invasively diagnose burn depth in a porcine model. Burns 2015;41:1242–52, doi:http://dx.doi.org/10.1016/j.burns.2015.03.001.
[38] Mazhar A, Saggese S, Pollins AC, Cardwell NL, Nanney L, Cuccia DJ. Noncontact imaging of burn depth and extent in a porcine model using spatial frequency domain imaging. J Biomed Opt 2014;19:086019, doi:http://dx.doi.org/10.1117/1.JBO.19.8.086019.
[39] Crouzet C, Nguyen JQ, Ponticorvo A, Bernal NP, Durkin AJ, Choi B. Acute discrimination between superficial-partial and deep-partial thickness burns in a preclinical model with laser speckle imaging. Burns 2015;41:1058–63, doi:http://dx.doi.org/10.1016/j.burns.2014.11.018.
[40] Kennedy GT, Stone R, Kowalczewski AC, Rowland R, Chen JH, Baldado ML, et al. Spatial frequency domain imaging: a quantitative, noninvasive tool for in vivo monitoring of burn wound and skin graft healing. J Biomed Opt 2019;24:1–9, doi:http://dx.doi.org/10.1117/1.JBO.24.7.071615.